HHS Public Access

Author manuscript

Comput Biol Med. Author manuscript; available in PMC 2022 September 01.

Published in final edited form as:

Comput Biol Med. 2021 September ; 136: 104723. doi:10.1016/j.compbiomed.2021.104723.

Computational modeling of nasal nitric oxide flux from the paranasal sinuses: validation against human experiment

Barak M. Spector[a], **Dennis J. Shusterman**[b], **Andrew N. Goldberg**[c], **Edward M. Weaver**[d], **Alexander A Farag**[a], **Bradley A. Otto**[a], **Kai Zhao**[a,*]

[a]Department of Otolaryngology - Head & Neck Surgery, the Ohio State University, Columbus, OH

[b]Upper Airway Biology Laboratory, University of California, San Francisco, CA

[c]Department of Otolaryngology – Head and Neck Surgery, University of California, San Francisco

[d]Department of Otolaryngology – Head and Neck Surgery, University of Washington, and Surgery Service, Seattle Veterans Affairs Medical Center, Seattle, WA

Abstract

Background: Nitric oxide (NO) is important in respiratory physiology and airway defense. Although the paranasal sinuses are the major source of nasal NO, transport dynamics between the sinuses and nasal cavities are poorly understood.

Methods: Exhaled nasal NO tracings were measured in two non-asthmatic subjects (one with allergic rhinitis, one without) using NO analyzer connected via face mask. We subsequently performed computational fluid dynamics NO emission simulations based on individual CT scans and compared to the experimental data.

Results: Simulated exhaled NO tracings match well with experimental data ($r>0.84$, $p<0.01$) for both subjects, with measured peaks reaching 319.6 ppb in one subject (allergic-rhinitis), and 196.9 ppb in the other. The CFD simulation accurately captured the peak differences, even though the initial sinus NO concentration for both cases was set to the same 9000 ppb based on literature value. Further, the CFD simulation suggests that ethmoid sinuses contributed the most (>67%, other sinuses combined <33%) to total nasal NO emission in both cases and that diffusion

*Corresponding author: Department of Otolaryngology–Head & Neck Surgery, The Ohio State University, 951 Olentangy River Road, Columbus, OH 43212., Phone: 614-293-3857, Fax: 614-293-7292, zhao.1949@osu.edu (K. Zhao).

Authorship contribution statement

Barak M. Spector: designed and performed the computational study, data analysis and wrote the original manuscript.

Dennis J. Shusterman: jointly conceptualized the study, provided experimental data for validation, performed data analysis and wrote the original manuscript draft, supervised and acquired funding and resources for the various stages of the project.

Andrew N. Goldberg: provided experimental data for validation, wrote, reviewed, and edited the final draft.

Edward M. Weaver: provided experimental data for validation, wrote, reviewed, and edited the final draft.

Alexander A Farag: wrote, reviewed, and edited the final draft.

Bradley A. Otto: wrote, reviewed, and edited the final draft.

Kai Zhao: jointly conceptualized the study, designed and performed the computational study, data analysis, wrote the original manuscript, supervised and acquired funding and resources for the various stages of the project.

Conflict of interest statement

The authors have no relevant financial interests or conflicts-of-interest to disclose.

contributes more than convective transport. By turning off diffusion (setting NO diffusivity to ~0), the NO emission peaks for both cases were reduced by >70%.

Conclusion: Historically, nasal NO emissions were thought to be contributed mostly by the maxillary sinuses (the largest sinuses) and active air movement (convection). Here, we showed that the ethmoid sinuses and diffusive transport dominate the process. These findings may have a substantial impact on our view of nasal NO emission mechanisms and sinus physiopathology in general.

Keywords

Nose; Diffusion; Nitric oxide; Paranasal sinuses

1. Introduction

Nitric oxide (NO) is a colorless, odorless gas that is produced from the amino acid arginine *in vivo* by three isoforms of the enzyme nitric oxide synthase (NOS). NO is present in exhaled breath, with concentrations in the upper respiratory tract (nasal NO or nNO) typically exceeding those in the lungs (fractional exhaled NO or FeNO)[1]. Moreover, the paranasal sinuses typically exhibit NO concentrations exceeding those derived directly from the nasal mucosa by 1–2 orders of magnitude[2,3], thereby serving as a “reservoir” of and major contributor to nNO. NO functions importantly in the respiratory system as bronchodilator [4], vasodilator [5], neurotransmitter [6,7], and as an immune modulator involved in regulation of inflammation[8,9] and in surveillance for neoplasia[10,11][12–15]. NO is also involved in the response to respiratory pathogens by upregulating mucociliary function [16–18]. Clinically, supplemental NO at levels exceeding physiologic values has been shown to benefit patients with acute respiratory distress syndrome (ARDS)[19] and both adults and newborns with pulmonary hypertension [20,21]. It is also currently being evaluated for the treatment of pulmonary hypertension occurring secondary to chronic obstructive pulmonary disease (COPD) and severe pneumonia associated with COVID-19[22]. Although NO production is increased with mucosal inflammation and allergic rhinitis, nNO is paradoxically low in chronic rhinosinusitis, potentially due to anatomically obstructed NO flux between the sinuses and nasal cavity [23]. nNO levels are also reduced in primary ciliary dyskinesia, as well as in most cases of cystic fibrosis [24].

Despite its important functional role, there is a lack of understanding of the dynamics of NO flux in the upper airway. One reason is the complexity of the human nose and sinus anatomy, which has high individual variability. The paranasal sinuses, which serve as major NO production site and reservoir, communicate with the nasal cavity through narrow openings - the ostia. The frontal, anterior ethmoid and maxillary sinuses open into a narrow ostiomeatal complex (OMC), with an average length of about 6mm and a diameter of 1–5mm (Proctor and Andersen, (1982)). The ostium size and geometry could serve as a limiting factor to upper airway NO dynamics. We previously conducted an observational study in which measured exhaled nNO levels were found to correlate significantly to the anatomical measurements of minimum OMC area based on CT scans in individuals with and without allergic rhinitis (n=33) [25]. Nevertheless, the details of this process or how each

sinus contributes to such emission process are not still well-understood, and nNO's utility in monitoring respiratory airway disease is still debated.

Sinus ventilation, by itself, has been an important topic in upper airway physiology, which has been historically measured by radioisotopes tracing with 133Xe [26] or 129Xe [27,28]. Typical time for washout of a healthy sinus ranges from 5–10 min. Due to the labor-intensiveness of these techniques, they are difficult to apply to a large patient population with increased health risk. Computational fluid dynamics modeling (CFD) is a method combines intensive computational methods with detailed geometric models and physical principles in order to simulate airflow and air ventilation. In the upper airway, it has been successfully utilized to model nasal aerodynamics[29,30], regional mucosal cooling[31], aerosol delivery[32], and anatomical transport of odorant molecules[33,34]. A few studies employing computational modeling of human nasal airflow and sinus gas exchange have also been performed, but they were mostly based on simplified anatomy[35] or focused primary on maxillary sinus[36]. These limited approaches are also largely theoretical without experimental data to validate[37].

With these limitations in mind, our goal for this study was to perform a computational fluid dynamics nasal sinus NO emission study based on individual nasal anatomy acquired from CT scans. Predictions of the time course of exhaled nNO were generated and compared to experimental data measured from the same individuals. Models were then perturbed to illustrate the key factors involved in NO sinus emissions.

2. Materials and methods

2.1. Study population

Two subjects, including a 37 year-old female with allergic rhinitis (subject 1) and a 41 year-old female with neither rhinitis nor allergic skin test reactivity (subject 2), were selected from a previously published study at the University of California, San Francisco (UCSF) [25]. Both subjects gave negative histories for chronic sinusitis, prior sinus surgery, asthma or other chronic cardiopulmonary conditions, current smoking, and continuous therapy with agents having antihistaminic or anticholinergic effects. In the source study, subjects underwent the following procedures in a single day: 1) computerized tomography (CT) scanning of the sinuses (using a Phillips "Brilliance" scanner with 0.625 mm axial cuts and coronal reconstruction); and 2) Exhaled nasal NO tracings measured using a NO analyzer (Sievers 280i) connected via a face mask (King System, Noblesville, IN, USA). During the 2^{nd} procedure, after acclimation, subjects were instructed to inhale orally through the mask (which is equipped with a NO-scrubbing filter on its intake), and then to exhale nasally through the mask with on-screen visual feedback to maintain a target flow rate of 5 L/min (Fig. 1A). Both flow and exhaled nasal NO concentrations were recorded in real-time during these maneuvers. Further details of subject recruitment, screening, and testing appear in a previous publication.[25] Neither of the subjects selected for this pilot validation study had accessory maxillary ostia on CT scanning.

De-identified data were conveyed in a blinded manner to the Otolaryngology Department at the Ohio State University (OSU) Medical Center utilizing a Data Transfer Agreement, approved by University of California, San Francisco Institutional review board.

2.2. CFD model

Individualized CFD nasal airway models were constructed based on the CT scan for each subject using methods described previously[33,38]. In brief, the scans were imported into the commercial software AMIRA (Visualization Sciences Group, USA) to extract nasal cavity geometry. After necessary segmentation, smoothing, and correction for artifacts, a three-dimensional surface geometry of the nasal airway was generated. Then a second software ICEM CFD (Ansys, Inc., USA) was applied to generate a computational mesh with 1.9 million (Subject 1) and 2.4 million (Subject 2) hybrid finite elements. Each sinus was separated from main airway and individual labeled so that NO concentration within each sinus could be independently monitored or manipulated (see Fig. 1).

Next, the nNO measurement procedure was replicated for each subject *in silico*. The simulation was split into 3 steps: a steady state (representing acclimation), a 5 second period with no nasal airflow (oral inhalation), and 10 seconds of nasal exhalation (NO sampling). The time period for each phase (5s and 10s) was determined based on the average values in sampled flow traces. The initial NO concentration in the sinuses and main nasal airway were set to 9000 ppb and 40.6 ppb, respectively, to represent their different NO production levels based on published *in vivo* measurements[3,24].

During the acclimation, expiratory quasi-steady laminar flows were simulated at pressure drop of 15 Pascal, representing restful breathing[39,40]. The simulations were converged once the residual of each variable was less than 10^{-5}. The numerical method and meshing protocol applied in this study has been previously validated against experimental measurements[41]. During the 5 second of oral inhalation phase, the nasal airflow velocity was set to 0 and the flow simulation was turned off since no air would flow in the nasal airway, however the time dependent NO mass transport simulation was still carried out with the sinus NO concentration replenished to the 9000 ppb, so that NO can continue to diffuse out the sinuses. The diffusivity of nitric oxide was set to 0.143 cm^2/s based on EPA estimation tool[42]. The value was conservatively set at the lower bound of the error range so that the contribution of the diffusive transport will be not over-estimated. Since the mass transport equation converged linearly, a fixed time step of 0.1s was applied for 50 steps (equals 5s).

For the final nasal exhalation and NO sampling phase, the air flow momentum/continuity equations were turned back on with an out-flow rate of 5 L/min assigned at the nasal pharynx plane. A time-dependent simulation for both airflow and NO diffusion was carried out using an adaptive time step scheme with initial time step set at 1e-5 s. NO concentration in each sinus, in the main nasal airway and at the nostrils were continuously recorded throughout all phases.

2.3. Data processing and analysis

In the source study, nNO had been measured utilizing a mask interface, resulting in a combined output from both nostrils. To match this experimental setup in the simulation, the bilateral exhaled NO concentrations were calculated by combining the modeled volumetric flow at each nostril normalized to the total volumetric flow rate. Predicted nNO was compared to the measured values for the 10 s period following onset of exhalation using Pearson correlation in SPSS based on 100 equally-spaced resampled time points (sampling rate of 10 Hz).

3. Results

Fig. 2A and B show the comparison of simulated vs. experimentally measured exhaled nNO tracings for both subjects. The measured exhaled NO concentrations rose sharply after the onset with peak reaching 319.6 ppb for Subject 1 and 196.9 ppb for Subject 2. The CFD simulation matched well with experimental data for both subjects with high correlation ($r > 0.84$, $p<0.01$) and accurately predicted the peak differences. Fig. 2C shows the NO concentration contours plots both in 3D and in a coronal plane that cuts across the ostiomeatal complex. During the initial second, the NO that had diffused to the main nasal airway during the previous oral inhalation phase was quickly washed out, which is likely responsible for the peak. Subsequent expiratory airflow continued to wash NO out from the middle to superior part of the nasal airway, regions where sinuses make connections with the main airway, which likely then produced the decaying and plateau phase of the NO tracing at the nostrils (see timing arrows and also S1 Video).

Fig. 3 A and B summarize the simulated NO concentrations in each sinus, which started to decrease during the oral inhalation (no nasal airflow) phase due to diffusion, which then accelerated during the nasal exhalation phase when convective transport further enhanced the diffusion transport. We also surprisingly found that ethmoid sinuses NO concentration decreased far more than the rest of the sinuses in both subjects, and contributed the most to total nasal NO emission (see Fig. 3C; >67%, other sinuses combined <33%, see also Table 1). We therefore set out to confirm this phenomenon by changing ethmoid sinus NO concentration to 0 and re-running the simulation. As shown in Fig. 2A and B, turning off ethmoid NO concentration resulted in significant reduction of NO peaks for both subjects (the simulated NO peak for Subject 1 reduced from 295.5 to 111.0 ppb or a 62.4% reduction, and for Subject 2 from 165.9 to 69.7 ppb, a 58.0% reduction), thereby confirming that ethmoid sinuses NO is the major contributor of exhaled NO concentration (at least for these two subjects).

Fig. 4 shows 3D plots of airflow pathlines and 2D velocity contour plots in the coronal plane that cuts across the ostiomeatal complex. On our simulation, we didn't observe any visible airflow pathlines that penetrated into any of the sinuses in either of the subjects (i.e., airflow velocity in all sinuses is close to 0), although the airflow velocity in the regions that connect the sinuses to the main airway is not 0 and air stream recirculation is noted, especially in the connecting region to maxillary and ethmoid sinuses. Combining the data from Fig.3 A and B, the emission of NO from the sinuses is likely initiated by a diffusion process (even in the absence of nasal airflow), followed by airflow washout of NO in the regions that connect the

sinuses to the main airway, since airflows do not appear to be directly entering sinuses nor directly transporting NO from the sinuses. The washout is potentially further enhanced by the airflow recirculation in that region.

At this point in our analysis, the question arose: “Which process, diffusion or convection (air flow), contributes more to the overall NO sinus emission?” To explore this, we reran the simulation by turning off diffusion (setting NO diffusivity to ~0), and showed that in Fig. 2A,B, the simulated NO peaks were reduced 69.9% f(rom 295.5 to 88.9 ppm) for Subject 1, and 80.5% (from 165.9 to 32.3 ppb) for the Subject 2, and the total NO emissions for both subjects were reduced by more than 60% (see Table 1: 61% for Subject 1 and 69% for Subject 2). The reduction is even more dramatic than turning off ethmoid sinus NO, suggesting that diffusion seems to be more critical to the NO emission, at least for these two subjects under the current experimental scheme.

4. Discussion

Nitric oxide serves important physiological functions in the respiratory system. However, despite the fact that the paranasal sinuses apparently serve as a major reservoir of NO (with concentrations typically exceeding lower airway by 2–3 orders of magnitude), there is limited understanding of how such a NO reservoir contributes to NO concentrations and functions in the respiratory airway. Based on a few previous modeling studies of human nasal airflow and sinus gas exchange, absent anatomical variants (e.g., accessory ostia in the maxillary sinuses), natural sinus ventilation is remarkably limited and may be unable to support the functional “reservoir” hypothesis. For example, Hood et al. (2009) constructed a simple geometry consisted of a large truncated cone as a maxillary sinus, joined to a rectangular channel as main airway by a short/straight tube representing the ostium. They varied the ostium diameter, length and the presence or absence of an accessory ostium, while validating the model using xenon as a tracer in a separate experiment (Rennie et al., 2011). They showed that the natural single-ostium sinus ventilation is remarkably slow unless the ostium is very large and concluded that diffusion from the maxillary sinuses alone could not explain the observed nNO levels. They proposed that the physiological consequence might be to preserve bacteriostatically high NO levels in the maxillary sinuses.

On literature review, we found no published studies in which individual anatomical models were compared with individual measured nNO levels. Most previous modeling approaches were largely theoretical without experimental data to validate, and mostly focused on the maxillary sinus. A combined *in vivo* (experimental) – *in vitro* (CFD) study was therefore a logical extension of existing work in this area. Here, we presented a computational modeling study that carefully replicated a published experimental protocol, based on individual CT scans from subjects upon whom nasal NO measurements were performed. In addition, rather than concentrating exclusively on the dimensions of the ostiomeatal complex, all sinuses were considered in the investigation. Two subjects were modeled, both females ranging in age from their late 30’s to early 40’s (one with allergic rhinitis and the other non-allergic, non-rhinitic). The simulation results matched extremely well with experimental data for both subjects and accurately captured their exhaled NO peak differences, even though the initial sinus NO concentration for both cases was set to the same 9000 ppb. While there is some

published evidence that NO production may be increased with mucosal inflammation and allergic rhinitis, this is an assertion that we could not address with an n=2 sample. However, we showed here that even without postulating differing inflammatory NO production, an accurate simulation of NO transport kinetics between the sinuses and the main nasal airway based on anatomical differences alone may account for much of the observed differences between subjects, regardless of rhinitis status. This finding reinforces the important role of NO transport kinetics between the sinuses and main airway in our understanding of airway NO dynamics.

As our simulation showed (Fig. 2 and 3), NO transport kinetics starts with NO diffusion from the sinuses to the main nasal airway (which first occurs in the oral inhalation phase in our experimental scheme), regardless of whether there exists nasal airflow. The NO concentration then begins to build-up in the main nasal airway, which is quickly washed out during the initial nasal exhalation phase and results in a sharp exhaled NO peak. Subsequent expiratory airflow continues to wash NO out from the middle to superior part of the nasal airway, regions where sinuses make connections with the main airway, which may further enhance the diffusion transport. This later process likely produced the decaying and plateau phase of the NO tracing at the nostril (Fig. 3A,B). Diffusion alone during the 5s oral inhalation with no nasal air movement only contributed to a small percentage (16–17%) of total NO sinus emission (see Table 1). However, we further showed that by turning off diffusion, the total NO emission from the sinuses dropped by more than 60% for both subjects. The reduction is more significant for frontal and sphenoidal sinuses (~97%) than for ethmoid sinuses (~58%, see Table 1). Therefore, even though both diffusive and convective transports are important components of NO sinus emission, we believe that the diffusion process is likely a more critical step. Since we found no evidence that airflow directly penetrates into the sinuses, in order for mass transfer to occur, NO needs to first diffuse out of the sinus cavity, before convective air movement can further transport it away. Since both subjects have un-operated narrow natural ostia, we speculate that for patients with larger ostium or with an accessory ostium or after surgery, the situation may be very different. If airflow can directly penetrate into sinuses, the convective transport may out-weight the diffusive transport. We would further speculate that, if we had a longer inhalation (or added a breath-holding phase), the longer initial diffusion would result in more NO built-up in the main airway and result in higher peak during initial nasal exhalation, but the plateau may be determined by different factors. In fact, we observed that even though the peak nNO is higher in subject 1, the total NO emission for subject 2 (54.2 nL) is actually higher than that of subject 1 (48.6 nL, see Table 1). This is also reflected in Figure 3 that total sinus NO emission is actually higher in subject 2 than subject 1. So a high nNO peak may only reflect a temporal emission dynamics but not necessarily the overall total nNO emission. Furthermore, we also observed that the left side sinuses of subject 1contributed more to NO emission, whereas right side of subject 2 contributed more. It is unclear why different side contributed differently in different subjects. One possibility is the individual nasal anatomical variations. Another possibility is the nasal cycle: the left side of subject 1 seems to be more open than the right side, while the right side of subject 2 is more open. These hypotheses await future studies to be validated.

Finally – and most importantly – our simulation surprisingly suggests that ethmoid sinus NO concentration contributed far more to the total nasal NO emission than the rest of the sinuses combined, which is confirmed by artificially turning off ethmoid sinus NO concentration (to 0). As shown in Fig. 2A,B, turning off ethmoid NO concentration resulted in significant reduction of NO peaks for both subjects (~60%). While this finding remains to be confirmed in larger future studies, we started a search for a plausible explanation. Reading the literature, we believe the reason of why most previous studies focused on maxillary sinuses appears to be an intuitive assumption that the maxillary sinuses have the largest volume, therefore they would have a bigger impact on overall upper airway NO status. However, as we calculated the sinuses volume based on our two models, while indeed maxillary sinuses volume is 4–6 times larger than the ethmoid sinuses, the ethmoid sinuses surface area is actually not that much smaller than that of maxillary sinuses (see Table 1), due to the numerous ethmoid cells. The surface-to-volume ratio of ethmoid sinuses (8.3 and 7.2, respectively) is actually 3–4 times higher than that of maxillary sinuses (2.2 and 2.6). Since NO is produced by the enzyme nitric oxide synthase on the mucosal surface, one would argue that perhaps the high surface area or high surface-to-volume ratio may be more predictive of the sinus contribution in NO production. A high surface-to-volume ratio would translate to a unit volume being supported by a larger surface area in NO productivity. Furthermore, while part of the ethmoid cells (anterior) shared the same ostiomeatal opening with the maxillary sinuses to the main airway with multiple anterior ethmoid cells open into this ostiomeatal complex, the posterior ethmoid cells have additional opening posteriorly to the main airway. The size of combined ethmoid openings to the main nasal airway in our models (1.08 and 1.26 cm^2 for Subjects 1 and 2, respectively) are significantly larger than that of the maxillary sinuses (0.27 and 0.47 cm^2). Their greater connection to the main nasal airway may be another reason why the ethmoid sinuses contributed more to NO emissions.

In summary, our model verified the potential utility of CFD as a tool for predicting *in vivo* nNO levels, and suggested the importance of ethmoid sinuses contribution and diffusion over convection. An obvious limitation of our study is the small sample size, rendering it a proof-of-concept pilot study. Since NO has important functions in the respiratory system, one would expect the *in vivo* NO level in the inspiratory airflow to be physiologically more important for lower airway function than that in the expiratory airflow. However, in contrast to the measurement of exhaled nNO (standardized by the ATS and ERS), techniques to measure nasopharyngeal NO during inhalation are still not available. Thus, prediction of NO level in inspiratory phase using CFD models may have potential future physiological values.

5. Conclusions

To our knowledge, this is the first study utilizing individual, anatomically based, CFD models to predict the time course of nNO during nasal exhalation in human subjects, comparing predictions with actual *in vivo* nNO measurements. Unexpectedly, we also found that modeled NO flux from the ethmoid sinuses exceeded that from the maxillary and other sinuses combined in both subjects and that diffusive transport contributed more to the process. If replicated in a larger sample, these observations may fundamentally change our view of nasal NO source allocation, dispersion and mixing, with corresponding implications for sinus physiopathology in general.

Supplementary Material

Refer to Web version on PubMed Central for supplementary material.

Funding

This research was supported by NIH NIDCD R01 DC013626 and R21 DC017530 to KZ and departmental support to DJS (with source study funding from the Flight Attendant Medical Research Institute). Dr. Weaver's effort was supported by the Veterans Affairs Puget Sound Health Care System, Seattle, WA; the contents do not represent the views of the United States Government.

References

1. Lundberg JO. Nitric oxide and the paranasal sinuses. Anat Rec (Hoboken). 2008;291: 1479–1484. doi:10.1002/ar.20782 [PubMed: 18951492]
2. Lundberg JO, Rinder J, Weitzberg E, Lundberg JM, Alving K. Nasally exhaled nitric oxide in humans originates mainly in the paranasal sinuses. Acta Physiol Scand. 1994;152: 431–432. doi:10.1111/j.1748-1716.1994.tb09826.x [PubMed: 7701944]
3. Lundberg JO, Farkas-Szallasi T, Weitzberg E, Rinder J, Lidholm J, Anggård A, et al.High nitric oxide production in human paranasal sinuses. Nat Med. 1995;1: 370–373. doi:10.1038/nm0495-370 [PubMed: 7585069]
4. Gaston B, Reilly J, Drazen JM, Fackler J, Ramdev P, Arnelle D, et al.Endogenous nitrogen oxides and bronchodilator S-nitrosothiols in human airways. Proc Natl Acad Sci U S A. 1993;90: 10957–10961. doi:10.1073/pnas.90.23.10957 [PubMed: 8248198]
5. Martínez C, Cases E, Vila JM, Aldasoro M, Medina P, Marco V, et al.Influence of endothelial nitric oxide on neurogenic contraction of human pulmonary arteries. Eur Respir J. 1995;8: 1328–1332. doi:10.1183/09031936.95.08081328 [PubMed: 7489799]
6. Belvisi MG, Stretton CD, Miura M, Verleden GM, Tadjkarimi S, Yacoub MH, et al.Inhibitory NANC nerves in human tracheal smooth muscle: a quest for the neurotransmitter. J Appl Physiol (1985). 1992;73: 2505–2510. doi:10.1152/jappl.1992.73.6.2505 [PubMed: 1362724]
7. Bai TR, Bramley AM. Effect of an inhibitor of nitric oxide synthase on neural relaxation of human bronchi. Am J Physiol. 1993;264: L425–430. doi:10.1152/ajplung.1993.264.5.L425 [PubMed: 7684571]
8. Laubach VE, Shesely EG, Smithies O, Sherman PA. Mice lacking inducible nitric oxide synthase are not resistant to lipopolysaccharide-induced death. Proc Natl Acad Sci U S A. 1995;92: 10688–10692. doi:10.1073/pnas.92.23.10688 [PubMed: 7479866]
9. Wei XQ, Charles IG, Smith A, Ure J, Feng GJ, Huang FP, et al.Altered immune responses in mice lacking inducible nitric oxide synthase. Nature. 1995;375: 408–411. doi:10.1038/375408a0 [PubMed: 7539113]
10. Lala PK. Significance of nitric oxide in carcinogenesis, tumor progression and cancer therapy. Cancer Metastasis Rev. 1998;17: 1–6. doi:10.1023/a:1005963400984 [PubMed: 9544419]
11. Xie K, Fidler IJ. Therapy of cancer metastasis by activation of the inducible nitric oxide synthase. Cancer Metastasis Rev. 1998;17: 55–75. doi:10.1023/a:1005956721457 [PubMed: 9544423]
12. Beckman JS, Beckman TW, Chen J, Marshall PA, Freeman BA. Apparent hydroxyl radical production by peroxynitrite: implications for endothelial injury from nitric oxide and superoxide. Proc Natl Acad Sci U S A. 1990;87: 1620–1624. doi:10.1073/pnas.87.4.1620 [PubMed: 2154753]
13. Gerlach H, Rossaint R, Pappert D, Falke KJ. Time-course and dose-response of nitric oxide inhalation for systemic oxygenation and pulmonary hypertension in patients with adult respiratory distress syndrome. Eur J Clin Invest. 1993;23: 499–502. doi:10.1111/j.1365-2362.1993.tb00797.x [PubMed: 8405003]
14. Puybasset L, Rouby JJ, Mourgeon E, Stewart TE, Cluzel P, Arthaud M, et al.Inhaled nitric oxide in acute respiratory failure: dose-response curves. Intensive Care Med. 1994;20: 319–327. doi:10.1007/BF01720903 [PubMed: 7930025]

15. Bove PF, van der Vliet A. Nitric oxide and reactive nitrogen species in airway epithelial signaling and inflammation. Free Radic Biol Med. 2006;41: 515–527. doi:10.1016/j.freeradbiomed.2006.05.011 [PubMed: 16863984]
16. Jain B, Rubinstein I, Robbins RA, Leise KL, Sisson JH. Modulation of airway epithelial cell ciliary beat frequency by nitric oxide. Biochem Biophys Res Commun. 1993;191: 83–88. doi:10.1006/bbrc.1993.1187 [PubMed: 7680560]
17. Runer T, Lindberg S. Effects of nitric oxide on blood flow and mucociliary activity in the human nose. Ann Otol Rhinol Laryngol. 1998;107: 40–46. doi:10.1177/000348949810700108 [PubMed: 9439387]
18. Runer T, Cervin A, Lindberg S, Uddman R. Nitric oxide is a regulator of mucociliary activity in the upper respiratory tract. Otolaryngol Head Neck Surg. 1998;119: 278–287. doi:10.1016/S0194-5998(98)70063-4 [PubMed: 9743084]
19. Rossaint R, Falke KJ, López F, Slama K, Pison U, Zapol WM. Inhaled nitric oxide for the adult respiratory distress syndrome. N Engl J Med. 1993;328: 399–405. doi:10.1056/NEJM199302113280605 [PubMed: 8357359]
20. Barnes PJ, Belvisi MG. Nitric oxide and lung disease. Thorax. 1993;48: 1034–1043. doi:10.1136/thx.48.10.1034 [PubMed: 7903007]
21. Lunn RJ. Inhaled nitric oxide therapy. Mayo Clin Proc. 1995;70: 247–255. doi:10.4065/70.3.247 [PubMed: 7861812]
22. Longobardo A, Montanari C, Shulman R, Benhalim S, Singer M, Arulkumaran N. Inhaled nitric oxide minimally improves oxygenation in COVID-19 related acute respiratory distress syndrome. Br J Anaesth. 2021;126: e44–e46. doi:10.1016/j.bja.2020.10.011 [PubMed: 33138964]
23. Rimmer J, Hellings P, Lund VJ, Alobid I, Beale T, Dassi C, et al.European position paper on diagnostic tools in rhinology. Rhinology. 2019;57: 1–41. doi:10.4193/Rhin19.410
24. Lundberg JO, Weitzberg E, Nordvall SL, Kuylenstierna R, Lundberg JM, Alving K. Primarily nasal origin of exhaled nitric oxide and absence in Kartagener's syndrome. Eur Respir J. 1994;7: 1501–1504. doi:10.1183/09031936.94.07081501 [PubMed: 7957837]
25. Shusterman DJ, Schick SF. Pilot evaluation of the nasal nitric oxide response to humming as an index of osteomeatal patency. American Journal of Rhinology. 2012;26: 4.
26. Zippel R, Streckenbach B. 133Xenon washout in the paranasal sinuses--a diagnostic tool for assessing ostial function. Rhinology. 1979;17: 25–29. [PubMed: 432473]
27. Kalender WA, Rettinger G, Suess C. Measurement of paranasal sinus ventilation by xenon-enhanced dynamic computed tomography. J Comput Assist Tomogr. 1985;9: 524–529. doi:10.1097/00004728-198505000-00022 [PubMed: 3989051]
28. Marcucci C, Leopold DA, Cullen M, Zinreich SJ, Simon BA. Dynamic assessment of paranasal sinus ventilation using xenon-enhanced computed tomography. Ann Otol Rhinol Laryngol. 2001;110: 968–975. doi:10.1177/000348940111001014 [PubMed: 11642432]
29. Keyhani K, Scherer PW, Mozell MM. Numerical simulation of airflow in the human nasal cavity. Journal of biomechanical engineering. 1995;117: 429–441. [PubMed: 8748525]
30. Subramaniam R, Richardson R, Morgan K, Kimbell J. COMPUTATIONAL FLUID DYNAMICS SIMULATIONS OF INSPIRATORY AIRFLOW IN THE HUMAN NOSE AND NASOPHARYNX. Inhalation Toxicology. 1998;10: 91–120. doi:10.1080/089583798197772
31. Zhao K, Jiang J, Blacker K, Lyman B, Dalton P, Cowart BJ, et al.Regional peak mucosal cooling predicts the perception of nasal patency: Mucosal Cooling and Nasal Patency. The Laryngoscope. 2014;124: 589–595. doi:10.1002/lary.24265 [PubMed: 23775640]
32. Schroeter JD, Kimbell JS, Asgharian B. Analysis of Particle Deposition in the Turbinate and Olfactory Regions Using a Human Nasal Computational Fluid Dynamics Model. Journal of Aerosol Medicine. 2006;19: 301–313. doi:10.1089/jam.2006.19.301 [PubMed: 17034306]
33. Zhao KEffect of Anatomy on Human Nasal Air Flow and Odorant Transport Patterns: Implications for Olfaction. Chemical Senses. 2004;29: 365–379. doi:10.1093/chemse/bjh033 [PubMed: 15201204]
34. Zhao K, Jiang J, Pribitkin EA, Dalton P, Rosen D, Lyman B, et al.Conductive olfactory losses in chronic rhinosinusitis? A computational fluid dynamics study of 29 patients: Conductive olfactory

losses. International Forum of Allergy & Rhinology. 2014;4: 298–308. doi:10.1002/alr.21272 [PubMed: 24449655]

35. Hood CM, Schroter RC, Doorly DJ. Computational modeling of flow and gas exchange in models of the human maxillary sinus. J Appl Physiol. 2009;107: 9.
36. Chung S-K, Jo G, Kim SK, Na Y. The effect of a middle meatal antrostomy on nitric oxide ventilation in the maxillary sinus. Respiratory Physiology & Neurobiology. 2014;192: 7–16. doi:10.1016/j.resp.2013.12.003 [PubMed: 24333403]
37. Kang I, Park S. Numerical study on nitric oxide transport in human nasal airways. J Mech Sci Technol. 2018;32: 1423–1430. doi:10.1007/s12206-018-0246-1
38. Zhao K, Pribitkin EA, Cowart BJ, Rosen D, Scherer PW, Dalton P. Numerical modeling of nasal obstruction and endoscopic surgical intervention: outcome to airflow and olfaction. American journal of rhinology. 2006;20: 308–316. [PubMed: 16871935]
39. Zhao K, Malhotra P, Rosen D, Dalton P, Pribitkin EA. Computational Fluid Dynamics as Surgical Planning Tool: A Pilot Study on Middle Turbinate Resection: CFD AND NASAL SURGERY. The Anatomical Record. 2014;297: 2187–2195. doi:10.1002/ar.23033 [PubMed: 25312372]
40. Zhao K, Jiang J. What is normal nasal airflow? A computational study of 22 healthy adults: Normal human nasal airflow. International Forum of Allergy & Rhinology. 2014;4: 435–446. doi:10.1002/alr.21319 [PubMed: 24664528]
41. Li C, Jiang J, Dong H, Zhao K. Computational modeling and validation of human nasal airflow under various breathing conditions. Journal of Biomechanics. 2017;64: 59–68. doi:10.1016/j.jbiomech.2017.08.031 [PubMed: 28893392]
42. EPA On-line Tools for Site Assessment Calculation. https://www3.epa.gov/ceampubl/learn2model/part-two/onsite/estdiffusion-ext.html.

Highlights:

- A first simulation of Nitric Oxide emission from all sinuses based on individual CT scans.
- The simulations match well with experimental measured nasal NO concentrations.
- Surprisingly, ethmoid sinuses and diffusive transport dominate the NO emission process.

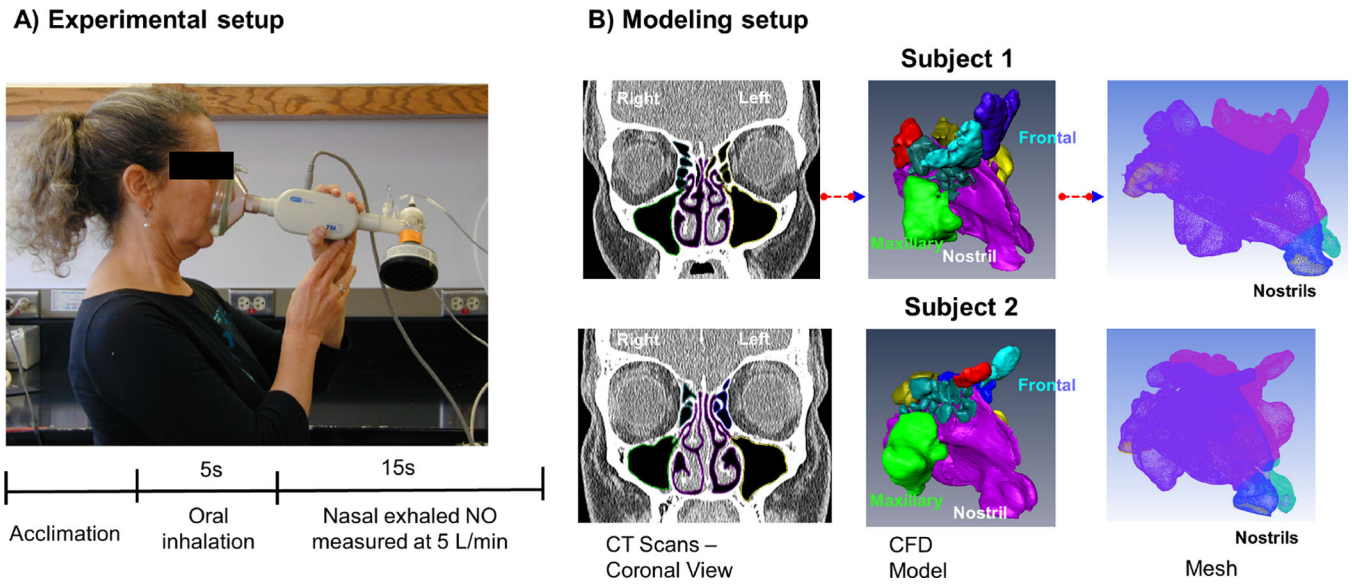

Figure 1.

A) Exhaled nasal NO tracings measured using a NO analyzer connected via a face mask. After acclimation, subjects were instructed to first inhale orally, and then exhale nasally through the mask with on-screen visual feedback to maintain a target flow rate of 5 L/min. B) Individualized CFD nasal airway models were constructed based on CT scans of one allergic rhinitic (subject 1) and one non-allergic, non-rhinitic subject (2). After necessary segmentation (1st panel), a three-dimensional surface geometry of the nasal airway was generated (2nd panel). Each sinus was separated from the main airway and individually labeled (color coded) so that NO concentration within each of the sinuses could be independently modeled or manipulated (3rd panel). Each nasal cavity was then filled with ~ 2 million hybrid finite elements.

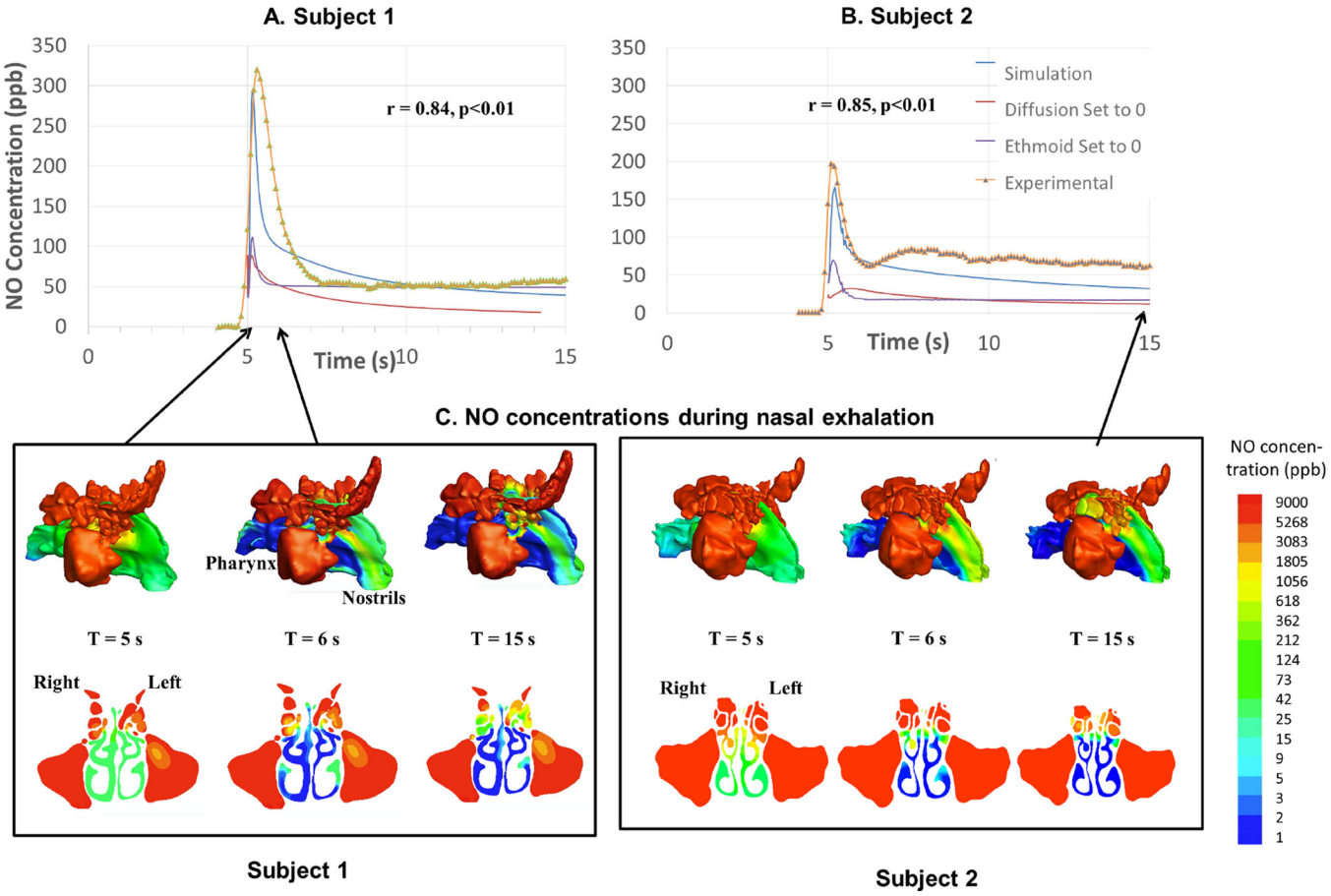

Figure 2.

A,B.) the comparison of simulated vs. experimental measured exhaled nasal nitric oxide (nNO) tracings for both subjects Measured nNO concentrations rise sharply after the onset of the exhalation with peaks reaching 319.6 ppb for Subject 1, and 196.9 ppb for Subject 2. The CFD simulation matched well with experimental data for both subjects with high correlation ($r > 0.84$, $p<0.01$) and accurately captured the peak differences. C.) NO concentration contours plots in log scale in 3D and in a cross-sectional coronal plane that cuts across the ostiomeatal complex.

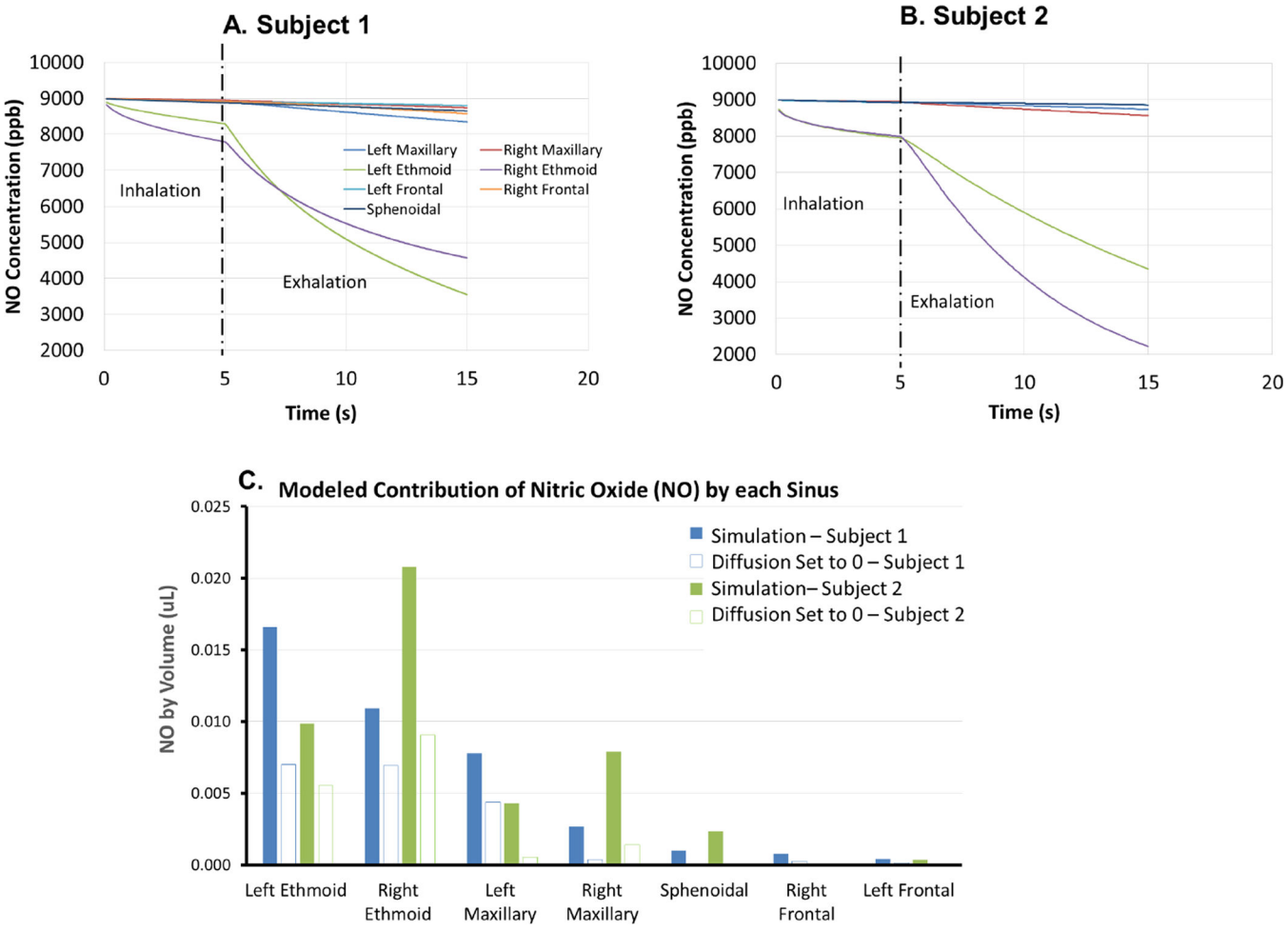

Figure 3.

The simulated NO concentrations in each sinus for A) Subject 1 and B) Subject 2, which started to decrease during the oral inhalation (no nasal airflow) phase, presumably due to diffusion, and then accelerated during the nasal exhalation phase when convective transport enhances diffusive transport. On simulation, we surprisingly found that ethmoid sinus NO concentration decreased far more than the rest of the sinuses, and C) contributed the most to total nasal NO emission in both cases (>67%, other sinuses combined <33%, see also Table 1).

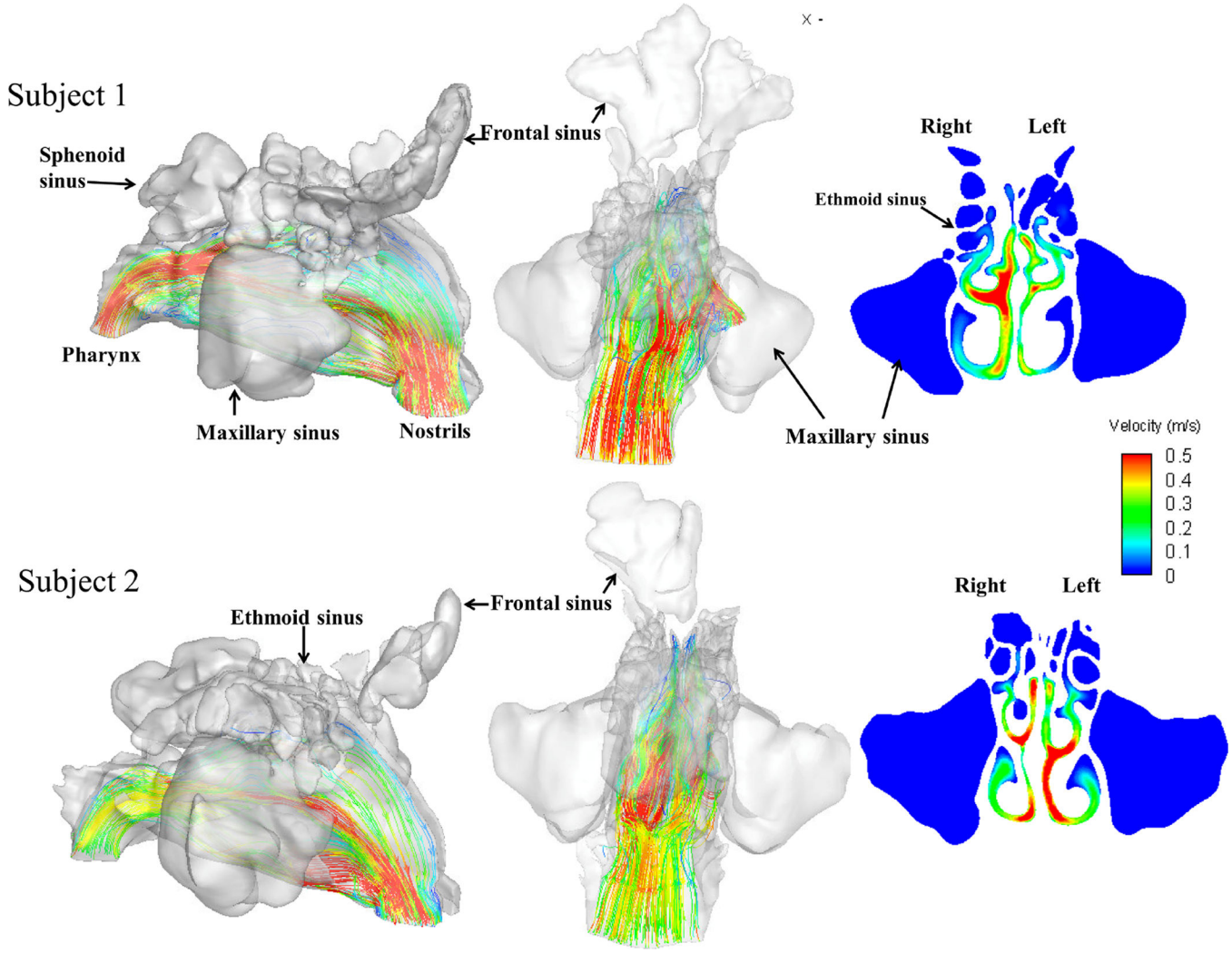

Figure 4.

3D plots of airflow pathlines and 2D velocity contour plots in the coronal plane that cut across the ostiomeatal complex. No visible pathline was observed that penetrated into any of the sinuses for either of the subjects (i.e., airflow velocity in all sinuses is close to 0). However the airflow velocity in the regions that connecting the sinuses to the main airway was not 0.

Table 1.

Nitric Oxide concentration in sinuses and volumetric data of sinuses

			Subject 1		Subject 2	
NO Emission (ppb*L or nL)			**Normal**	**Diffusion "Turned off" & % reduction**	**Normal**	**Diffusion "Turned off" & % reduction**
Maxillary	**Left**	**Inhalation**	1.2		1.1	
		Exhalation	7.8	4.4	4.3	0.5
	Right	**Inhalation**	0.5		1.1	
		Exhalation	2.7	0.4	7.9	1.4
	L+R % of total	**Inhalation**	20%	−61%	25%	−87%
		Exhalation	26%	25%	27%	12%
Ethmoid	**Left**	**Inhalation**	2.4	−63%	2.5	−55%
		Exhalation	16.6	7.01	9.8	5.6
	Right	**Inhalation**	3.6	−52%	2.8	−62%
		Exhalation	10.9	6.93	20.8	9.1
	L+R % of total	**Inhalation**	**70%**	−58%	**61%**	−59%
		Exhalation	**69%**	**73%**	**67%**	**88%**
Frontal	**Left**	**Inhalation**	0.4		0.3	
		Exhalation	0.4	0.1	0.3	0.02
	Right	**Inhalation**	0.1		0	
		Exhalation	0.8	0.2	0	0
	L+R % of total	**Inhalation**	6%	−77%	4%	−97%
		Exhalation	3%	2%	1%	0%
Sphenoidal		**Inhalation**	0.3		0.9	
		Exhalation	1.0	0.0006	2.3	0.09
	L+R % of total	**Inhalation**	4%	−100%	10%	−97%
		Exhalation	2%	0%	5%	1%
Total NO Emission		**Inhalation**	8.4	−61%	8.7	−69%
		Exhalation	40.1	19.1	45.5	16.6
		Inhalation %	17%		16%	
	Inhalation+Exhalation		48.6		54.2	
Ethmoid Volume (ml)	**Left**		3.5		2.7	
	Right		3.4		3.6	
	total		6.9		6.3	
Ethmoid Surface Area (cm^2)	**Left**		23.3		24.3	
	Right		26.5		28.4	
	total		49.8		52.7	
Maxillary Volume (ml)	**Left**		13.8		21.1	
	Right		12.5		21.1	
	total		26.3		42.2	

			Subject 1		Subject 2	
NO Emission (ppb*L or nL)			**Normal**	**Diffusion "Turned off" & % reduction**	**Normal**	**Diffusion "Turned off" & % reduction**
Maxillary Surface Area (cm^2)	**Left**		35.1		45.6	
	Right		33.3		46.0	
	total		68.3		91.6	
Ethmoid Surface Area to Volume Ratio			7.2		8.3	
Maxillary Surface Area to Volume Ratio			2.6		2.2	
Ethmoid opening size (cm^2)	**Left**		0.37		0.61	
	Right		0.71		0.65	
	total		1.08		1.26	
Maxillary opening size (cm^2)	**Left**		0.17		0.21	
	Right		0.10		0.26	
	total		0.27		0.47	